

DOI: 10.19615/j.cnki.1000-3118.170922

## New fossils of paraceratheres (Perissodactyla, Mammalia) from the Early Oligocene of the Lanzhou Basin, Gansu Province, China

LI Yong-Xiang<sup>1</sup> ZHANG Yun-Xiang<sup>1\*</sup> LI Ji<sup>2,3</sup> LI Zhi-Chao<sup>1</sup> XIE Kun<sup>1</sup>

(1 State Key Laboratory of Continental Dynamics, Department of Geology, Institute of Cenozoic Geology and Environment, Northwest University Xi'an 710069 \* Corresponding author: yxzhang@nwu.edu.cn)

(2 Institute of Silk Road Studies, Northwest University Xi'an 710069)

(3 Northwest Institute of Historical Environment and Socio-Economic Development, Shaanxi Normal University Xi'an 710119)

**Key words** Lanzhou Basin, Early Oligocene, Paraceratheriidae, new species

**Citation** Li Y X, Zhang Y X, Li J et al., 2017. New fossils of paraceratheres (Perissodactyla, Mammalia) from the Early Oligocene of the Lanzhou Basin, Gansu Province, China. Vertebrata PalAsiatica, 55(4): 367–381

### Summary

This paper describes a new species of paraceratheres: *Paraceratherium huangheense* sp. nov., which was excavated from the yellow sand layers at the bottom of the Early Oligocene Hanjiajing Formation of the Lanzhou Basin, Gansu, China. The paleomagnetic age of the strata is about 31.5 Ma.

### Order Perissodactyla Owen, 1785

#### Superfamily Rhinocerotoidea Owen, 1845

#### Family Paraceratheriidae Osborn, 1923

#### Subfamily Paraceratheriinae Osborn, 1923

#### *Paraceratherium* Forster-Cooper, 1911

#### *Paraceratherium huangheense* sp. nov.

(Figs. 1–3; Tables 1–3)

**Holotype** NWUV 1479, a right mandible with the all right cheek tooth, symphyseal part and two lower incisors.

**Referred specimens** NWUV 1480, a part of left maxilla with P2–P4; NWUV 1481, left M2; NWUV 1482, right M3; two left (NWUV 1484–1485) and one right (NWUV 1483) mandibles with m1–m3; NWUV 1486, a left incisor.

**Etymology** The specific name refers to “Huanghe” River, where the new species were discovered nearby.

**Locality and age** Lanzhou Basin, Gansu Province; Early Oligocene Hanjiajing

国家自然科学基金重大项目(批准号: 41290253)资助。

收稿日期: 2017-5-16

Formation.

**Diagnosis** A large paraceratherium. A pair of the first lower incisor (i1) with asymmetrically conical crown, separated by a short diastema, and extended slightly upward. It is without tooth trace on the diastema before P2. The ventral border of the horizontal ramus of the mandible is straight below the molars, but pronouncedly concave below the diastema. Mandibular angle angular, and the posterior border of ascending ramus slanted posteriorly. The mental foramen located below p3. Dental formula: ?·?·3·3/1·0·3·3.

**Description Upper Dentition** The length of fragmental maxilla (Fig. 1A, NWUV 1480) is 210 mm with maximum height of 160 mm. There is no trace of tooth socket anterior to P2, and the diastema anterior to P2 is clearly convex. P2 is triangular, wider than long. The tooth has continuous enamel on labial and lingual sides, but lacks enamel on the posterior wall, where it closely contacts P3. Crown surface of P2 is heavily worn, almost flat and only slightly uneven on the posterior part. P3 is irregularly quadrilateral with labial border longer than lingual one, and the width is greater than the length. Parastyle is prominent. Enamel is present on both buccal and lingual sides. A small medifossette is present in the middle of the crown. P4 is similar to P3, but the parastyle is more prominent, and the cingulum is absent on the distal half of the lingual side. The P4 is closely appressed to P3, and larger than latter.

M2 (Fig. 1B, NWUV 1481) is trapezoid in outline with the buccal border as long as the lingual one, and becomes slightly narrower distally. Parastyle is very prominent and parastyle fold is shallow. Buccal wall on metacone is strongly convex. Protoloph is long and extends to the lingual side. The antecrochet is large and broadly V-shaped, extending distally to the mesial wall of metaloph and dividing the medifossette into lingual and buccal parts. Metaloph is slightly wider and shorter than protoloph, and hypocone is smaller than protocone. Crochet is low. Labial cingulum is low at the base of the paracone but highly-ridged at the base of the metacone.

M3 (Figs. 1C, 2, NWUV 1482) is triangular with the vestigial, highly reduced posterior end of ectoloph. Parastyle and the lingual ends of the protolophs and metalophs are damaged. A wide uplift under the protoloph extends to the medisinus and meet at the uplift from base of the metaloph. Anterior cingulum is highly-ridged and gradually reduced from lingual to labial side. Posterior cingulum is developed distal to the base of the hypocone, lowest at the base of the metacone, and rises to the labial side. The main cusps, including the protocone, hypocone, paracone, metacone, and parastyle, bear robust roots.

**Lower dentition** A right mandible with the symphyseal region (Fig. 1D, NWUV 1479) preserves a pair of the first incisors and the cheek teeth on right side, but the angle and ascending ramus are not complete. The symphyseal region of mandible is similar to that of *Paraceratherium bugtiense* described by Forster-Cooper (1911), but is obviously larger and thicker. Two lower incisors (i1) are not close to each other, conically-shaped, and extend slightly upward. The ventral border of the horizontal ramus of the mandible is straight below the molars, but pronouncedly concave below the diastema. The mental foramen is situated below p3 and about at the level of the half height of the ramus. Dental formula is

?·?·3·3/1·0·3·3. Mandibular angle is angular (Fig. 1F, NWUV 1483), and the posterior border of ascending ramus is slanted posteriorly.

The i1 (Fig. 3, NWUV 1486, unworn) is similar to that of *Dzungariotherium orgosense* described by Qiu et al. (2004), but is slightly smaller. On the heavily-worn specimen (Fig. 1D, NWUV 1479), the upper ridge is weak.

The p2 (Fig. 1D, NWUV 1479) is small and single-rooted. Due to the heavily-worn condition, crown surface is almost flat and the enamel is only surrounded on anterior, posterior and buccal walls. Crown is mesiodistally elongated. The labial cingulum is developed.

The crown of p3 (Fig. 1D) is roughly trapezoid in outline with mesial border wider than the distal one. Only remnant talonid basin is present on crown, and the ectoflexid is a low groove. The labial cingulum is complete, whereas only posterior part of the lingual cingulum remains.

The p4 (Fig. 1D) is heavily worn, and the talonid basin is shallowly U-shaped. Protolophid, hypolophid and metalophid are very wide, whereas the entolophid tapers toward the lingual side. The ectoflexid is a wide, shallow valley. The cingulum is developed on labial and lingual sides.

The m1 is heavily worn (Fig. 1D). The trigonid basin is only a faint trace in the lingual, and the talonid basin is a shallow V-shaped valley, the ectoflexid is a flat wide V-shaped concave. The protoconid and the metaconid are expanded, and the paraconid is minimal. Both the outside hypoconid and the inside endoconid are heavily worn to root. Labial cingulum is development in the ectoflexid.

The m2 is mild worn and the crown surface is remained (Fig. 1D). The paralophid is very thin, while the metalophid and the entolophid are thick. The trigonid basin and the talonid basin are all U-shaped but the former is shallow and the latter deep. The ectoflexid is shallow V-shaped. Labial cingulum is high in the anterior and low in the posterior.

The m3 is the lightest worn, and the crown surface morphology is similar to m2 (Fig. 1D). Compared to m2, its talonid basin is wider, ectoflexid is deeper and ridges are slightly narrower. Labial cingulum is developed only in the antero-labial corners and the postero-wall of the entolophid.

**Comparison and discussion** The genus *Paraceratherium* was established from a mandible from Baluchistan (in southern Pakistan) by Forster-Cooper in 1911. Its features were given by Forster-Cooper (1911) as: “the generic characters relied upon being the very unusual position and shape of the two lower incisors”, “The chief peculiarity of the jaw lies in the shape and position of the single stout incisor in each ramus.” Beneath the molars the contour is flat, but below the diastema in between p2-i1 is concave, and stretching anteriorly together with the incisor (i1).

According to Qiu and Wang (2007), besides type species *P. bugtiense*, there are three valid species of *Paraceratherium*: *P. asiaticum* (=*Indricotherium transouralicum*), *P. grangeri* and *P. lepidum* (Fig. 4B–E).

Morphologically, the above described specimens of *P. huangheense* from the Lanzhou Basin are almost identical to those of *Paraceratherium*: a single stout incisor in each ramus

and stretching forward (Fig. 4). But there are some differences between *P. huangheense* and the other species (Fig. 4; Table 4).

*P. huangheense* is similar to *P. bugtiense* (Fig. 4B) in the following features: loss of P1; triangular form of P2; below the diastema in between p2–i1 is concave; single root of p2; the mandibular angle is angular. On the other hand, *P. huangheense* is distinguished from *P. bugtiense* (features in brackets) by its larger size, mental foramen underlies p3 (p2), the posterior border of ascending ramus posteriorly slanted (vertical), and a short diastema between the bases of i1 (closely appressed) (Forster-Cooper, 1911; Gromova, 1959).

*P. huangheense* is similar to *P. asiaticum* (Fig. 4C) only in two following features: loss of P1 and a single stout incisor in each ramus extend forward. However, their differences are greater. *P. huangheense* is different from *P. asiaticum* (features in brackets) by its larger size (p2–m3 77% as long as that of *P. huangheense*; Gromova, 1959:89), below the diastema in between p2–i1 the contour is concave (not concave), mandibular foramen underlies p3 (p2), mandibular angle is angular (rounded), slanting upward side posterior border of ascending ramus (anteriorly slanted), and the outline of P2 crown is roughly triangular (trapezoid) (Borissiak, 1923; Gromova, 1959, Qiu and Wang, 2007).

*P. huangheense* is similar to *P. grangeri* (Fig. 4D) in the following features: size close to each other, loss of P1, and a single stout incisor in each ramus and extend forward. But they have some differences as follow. *P. huangheense* is distinguished from *P. grangeri* by its mandibular angle is angular (rounded), the posterior border of ascending ramus is slanted posteriorly (convex posteriorly), the outline of P2 crown is triangular (trapezoid), p2 is single-rooted (double-rooted), below the diastema in between p2–i1 is concave (without or weakly concave), and dental formula ?·?·3·3/1·0·3·3 (1·1·4·3/1·0·3·3) (Osborn, 1923; Granger and Gregory, 1936).

*P. huangheense* is similar to *P. lepidum* (Fig. 4E) in the following features: size close to each other, loss of P1, triangular form of P2, below the diastema in between p2–i1 is concave; single root of p2; and a single stout incisor in each ramus and stretching forward. But the main characteristics of *P. lepidum* are distinct from *P. huangheense* in having a wide and deep notch (incisura vasorum) anterior to the mandibular angle on the ventral border of the horizontal ramus (Fig. 4E) (Qiu and Wang, 2007).

In recent years, some giant rhinoceroses have been reported from the Late Oligocene of north-central Anatolia by Antoine et al. (2008), and from Oligocene and Middle Miocene deposits of the Kagizman-Tuzluca Basin, Eastern Turkey by Sen et al. (2011). These fragmental limbs are identified as the *Paraceratherium* sp.

Based on the comparisons (Fig. 4; Table 4), it is clear that the *P. huangheense* from Lanzhou is very similar to *P. bugtiense* from Dera Bugti, Baluchistan, indicating they may have a close phylogenetic relationship. Furthermore, the paleomagnetic age of the layer bearing *P. huangheense* in the Lanzhou Basin is 31.5 Ma (Yue et al., 2001; Zhang, 2015), implying that the bed bearing *P. bugtiense* from Baluchistan is probably also Early Oligocene, which is consistent with two Early Oligocene cricetids from the same *Paraceratherium*-layer

in Baluchistan (Marivaux et al., 1999).

Giant rhino fossils from the Lanzhou Basin are the main evidence to show that during the Oligocene giant rhinos lived in north-western China, north of the Tibetan Plateau, while they were also distributed in the Indo-Pakistan subcontinent to the south of the Tibetan Plateau. This distribution indicates that the elevation of the Tibetan Plateau was not high enough to prevent exchanges of large mammals. Giant rhinos, the rhinocerotid *Aprotodon*, and chalicotheres still dispersed north and south of “Tibetan Plateau” (Qiu et al., 2001; Deng and Ding, 2015). The results of this paper show clearer evidence to prove the existence of the *P. Huangheense* in the Lanzhou Basin of China during the Early Oligocene around 31.5 Ma, whose fossils are very similar to the *P. bugtiense* from Dera Bugti of Baluchistan.

## 兰州盆地新发现的早渐新世巨犀化石

李永项<sup>1</sup> 张云翔<sup>1</sup> 李冀<sup>2,3</sup> 李智超<sup>1</sup> 谢坤<sup>1</sup>

(1 西北大学大陆动力学国家重点实验室, 地质学系, 新生代地质与环境研究所 西安 710069)

(2 西北大学丝绸之路研究院 西安 710069)

(3 陕西师范大学西北历史环境与经济社会发展研究院 西安 710119)

**摘要:** 描述了在兰州盆地渐新统韩家井组底部的黄砂层中新发现的巨犀化石: 黄河巨犀 (*Paraceratherium huangheense* sp. nov.) (新种), 该化石产出层位的古地磁年龄为距今31.5 Ma。新种主要特征为: P2之前无齿槽痕迹, 一对下门齿粗壮, 互相靠近, 向前平伸且略微上翘, 下颏孔位于p3之下, 水平支下缘平直, p2前的齿隙部分向上隆起, 下颌角圆钝, 上升支后缘斜向后上方, 齿式: ?·?·3·3/1·0·3·3。除个体较大、下颌后缘有所不同之外, 其下颌的总体特征与巴基斯坦的*Paraceratherium bugtiense*最为接近, 显示两者可能具有较近的亲缘关系。新标本的发现为确定经典的Dera Bugti地点产大巨犀化石层位的年代提供了新的证据, 并为青藏高原的隆升讨论提供了新的哺乳动物化石证据。

**关键词:** 兰州盆地, 早渐新世, 巨犀, 新种

中图法分类号: Q915.877 文献标识码: A 文章编号: 1000-3118(2017)04-0367-15

### 1 研究背景

兰州盆地新生代早期的地层有不同的划分。盆地的新生界最早被称为甘肃建造, 包括长川子系、咸水河系、观音寺系和五泉山系(Young and Bien, 1937)。咸水河系的时代最初被认为是中新世。邱占祥等(邱占祥等, 1997; Qiu et al., 2001)根据野外考察及相关研究, 将咸水河组分为下中上三段, 其下段的时代为渐新世, 中、上段分别为早、中中新世。下段包括南坡坪动物群和峡沟动物群, 中段包括张家坪动物群和对亭沟动物群, 上段包括泉头沟动物群和邢家湾动物群。后颉光普(2004)对兰州盆地的第三系又作了进一步划分, 并新建了许多岩组, 将含南坡坪动物群和峡沟动物群的地层分别划分为早渐

新统韩家井组和晚渐新统甘家滩组。韩家井组主要以灰白色、灰黄色砂岩为主，见大量红色泥砾及槽状交错层理，在该组的底部发现巨犀及一些啮齿类化石；甘家滩组则主要为棕红色粘土岩、砂质泥岩。沉积相分析显示该区渐新世早期为湖泊沉积，之后出现河流沉积环境，后期又过渡为湖泊沉积。

1964年，甘肃省地质局第四区测队在兰州盆地皋兰县李麻沙沟的黄砂岩(产南坡坪动物群)中首次采集到1件不完整的巨犀下颌骨化石，当时定为*Paraceratherium* sp.，时代为早渐新世。后中国科学院古脊椎动物与古人类研究所与甘肃省博物馆组成的联合考察队于1987和1995年分别在张家坪和烟筒沟附近从老乡手中收集到一些巨犀牙齿，据采集者描述，化石产自第一白砂岩层(张家坪动物群)。联合考察队在桃湾沟的第一白砂岩层中还发现了一些巨犀的肢骨(1995年)，定名为*Turfantherium elegans*，时代为早中新世早期(邱占祥、王伴月，2007)。

2013年在兰州市黄河以北黄羊头村附近渐新统韩家井组底部地层(李智超等，2016)中采集到一批巨犀化石，主要包括一件残破的左上颌骨带P2-P4和三件不完整的下颌骨以及部分头后骨骼等，代表了巨犀属(*Paraceratherium*)中一个新种。古地磁分析表明，韩家井组底界地层年龄约为31.5 Ma (Yue et al., 2001; 张鹏，2015)。

巨犀类颊齿冠面的术语及测量方法主要依据邱占祥、王伴月(2007)。NWUV，西北大学新生代地质与环境研究所脊椎动物标本编号；IVPP V，中国科学院古脊椎动物与古人类研究所脊椎动物化石编号。

## 2 化石记述

### 奇蹄目 *Perissodactyla* Owen, 1785

#### 犀超科 *Superfamily Rhinocerotoidea* Owen, 1845

#### 巨犀科 *Family Paraceratheriidae* Osborn, 1923

#### 巨犀亚科 *Subfamily Paraceratheriinae* Osborn, 1923

#### 巨犀属 *Paraceratherium* Forster-Cooper, 1911

#### 黄河巨犀(新种) *Paraceratherium huangheense* sp. nov.

(图1-3; 表1-3)

**正型标本** 一件较完整右下颌，保存联合部及完整右侧齿列，下颌角和垂直支部分缺失，NWUV 1479。

**归入材料** 左上颌带P2-P4, NWUV 1480; 左M2, NWUV 1481; 右M3, NWUV 1482; 一右下颌带m1-m3, NWUV 1483; 两左下颌带m1-m3, NWUV 1484-1485 (其中NWUV 1484残破，可能与NWUV 1479-1480为同一个体); 左下门齿, NWUV 1486。

**种名释义** 种名来自汉语拼音Huanghe，意为黄河，化石产地靠近黄河。

**产地和层位** 甘肃省兰州盆地，下渐新统韩家井组。

**特征** 大型巨犀，P2之前无齿槽痕迹，上颌齿隙部分明显上凹。下门齿(i1)一对，呈不对称截锥形，互相靠近，但留有齿隙，前伸，略微上翘。下颌吻部粗壮，水平支下缘平直，前部在p2前的齿隙下方向上凹入。下颌角角状，垂直支后缘斜向后上方。下领

孔位于p3之下。齿式：?·?·3·3/1·0·3·3。

**描述** 左上颌(NWUV 1480, 图1A)保存长度约210 mm, 高度约160 mm。牙齿磨蚀程度高, 应为老年个体。唇侧齿冠保留较多, 舌侧保留较少, 齿冠中部几乎磨平, P2只有珐琅质轮廓, P3和P4有珐琅质中窝残存。唇侧视, 3个前臼齿齿根粗壮清楚, 齿根除近根尖部分外, 大部分裸露。牙齿从前向后逐渐增长。P2之前无齿槽痕迹, 上颌齿隙部分明显向上凹入。牙齿唇侧齿带明显, 前后两端升高, 中部低平, 前部较弱而后部粗壮。P2两个齿根大小相近, P3–P4前齿根明显比后齿根粗壮。P2–P4, 前齿根趋于增大而后齿根逐渐变弱。残存的上颌骨外侧面由于齿根影响而明显凹凸不平, 总体呈一向外凸出的弧形。舌侧视, 齿冠很低, P2齿冠最高处为5 mm, P4中部最高处为18 mm; 齿根露出较多: P2–P4依次为21, 32, 38 mm, 除P2外, P3–P4未见舌侧齿根前后分叉。

P2冠面近于等腰三角形, 唇侧宽而舌侧窄, 前缘向后内方延伸, 后缘与P3紧密接触, 但接触边缘很不规则, 且缺失珐琅质层; 唇舌两侧牙齿边缘有薄而明显的珐琅质层, 冠面几乎磨平, 仅在中后部略有起伏变化。P3冠面呈宽大于长、唇侧较舌侧长的不规则四边形, 前附尖向前突出, 在唇舌两侧珐琅质层保留较多, 在齿冠中心有小的珐琅质中窝残存, 舌侧后部可见不规则的齿带残留。齿冠唇舌两侧较高, 中部明显凹下。P4紧靠P3, 形态与其类似, 但更大, 前附尖更突出, 舌侧后部未见齿带残留。

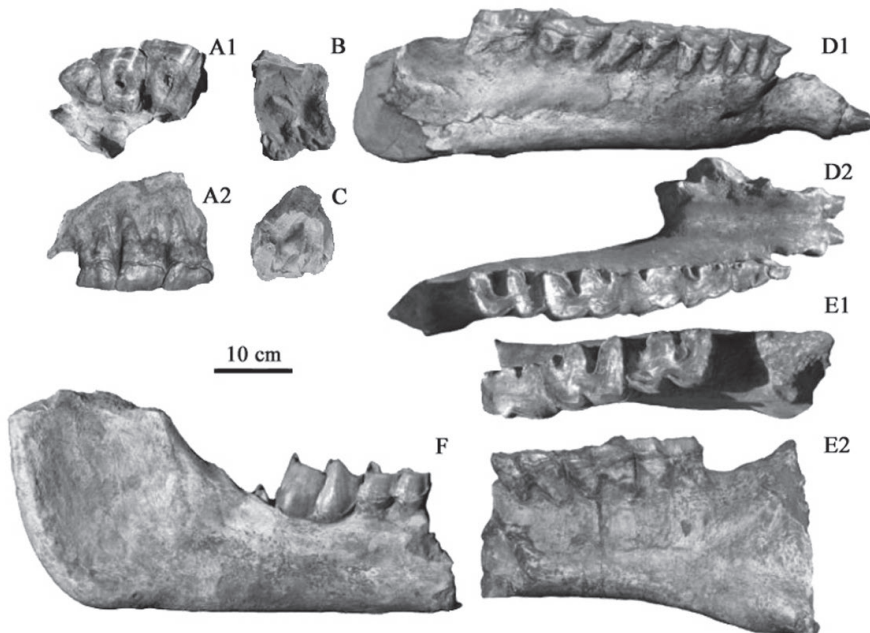


图1 黄河巨犀(新种)

Fig. 1 *Paraceratherium huangheense* sp. nov.

A. a part of left maxilla with P2–P4 (NWUV 1480) in ventral (A1) and labial (A2) views; B. left M2 (NWUV 1481) in occlusal view; C. right M3 (NWUV 1482) in occlusal view; D. a right mandible with the all right cheek teeth, symphyseal part and two lower incisors (NWUV 1479) in labial (D1) and occlusal (D2) views;

E. left mandibles with m1–m3 (NWUV 1485) in occlusal (E1) and labial (E2) views;

F. right mandibles with m1–m3 (NWUV 1483) in labial view

M2 (NWUV 1481, 图1B)磨蚀程度比NWUV 1482略浅，也是老年个体。标本前宽后窄，唇舌侧长度大致相当，牙齿前后缘中部略呈弧形向前弯，总体轮廓呈一弯曲梯形。前附尖伸向前方，前附尖沟浅。外壁在后尖处向外突出，原脊长，在舌侧膨大，由于磨蚀程度深，在舌侧基部与后脊相连；反前刺从原脊中部呈底部宽阔的V字形向后伸出，抵达后脊前壁，将中沟分为内外两部分。后脊比原脊略微宽短，并在舌侧收缩，前刺低矮。外齿带在前尖处低，到后尖处升高，中部低。

M3 (NWUV 1482, 图1C, 2)冠面轮廓为三角形。前附尖、原尖和次尖均有不同程度破损。外脊与后脊愈合为外后脊，其外后壁圆隆，不呈角形，中部略微鼓起。原脊中部下方，有一宽缓的隆起伸向中谷，在近谷口处与后脊基部下延并前伸的隆起相会合。前齿带高，从舌侧向唇侧逐渐降低，在原尖处齿带最高达26 mm, 至前尖处减至14 mm。后齿带在次尖外下方略强，在后尖外下方最低，然后向唇侧方向升起。在主要齿尖，包括原尖、次尖、前尖、后尖以及前附尖下方，均有粗壮的齿根支撑，其中前尖和前附尖、原尖和次尖下方的齿根分别相连甚至愈合近于板状，只有后尖下方的齿根呈独立柱状。

已保存的上牙材料未见M1，推测上牙齿式可能为：1(?)·0(?)·3·3。三件标本磨蚀程度不等，三个前臼齿磨蚀程度非常高，M2次之，应为老年个体，M3 (图2)磨蚀较轻，齿冠高度在后尖处达到最高，约为66 mm (包括齿带)。这3件上牙标本有可能代表3个不同年龄的个体。从3个前臼齿的形态上看，P2半臼齿化，P3-P4臼齿化。

下颌(NWUV 1479, 图1D)右侧下颌角处残破，上升支缺失，右侧齿列完整；左侧联合部及门齿保留，其余缺失。侧面视，门齿截锥状，下缘上翘，p2前的齿隙部分整体向上隆起，联合部下缘在此处向上弯曲，水平支下缘自p2下部开始向后基本平直，向前在齿缺部分向上凹入。下领孔位于p3齿根下方颌骨的中部。颊齿齿根大部外露，齿冠磨蚀

从后向前逐渐加深，至p2已基本磨平。嚼面视，双侧下门齿略向外斜伸。联合部在p2之前变窄，顶面为纵凹槽状，其后缘与m1前缘平齐。下牙齿式为1·0·3·3。下领角角状(NWUV 1483, 图1F)，上升支后缘斜向后上方。

左下门齿的齿冠未磨蚀时的形态接近于邱占祥等(2004)记述的*Dzungariotherium orgosense*, 但尺寸略小。齿冠断面椭圆形，舌面微凹，唇面略凸。侧面视，上缘近齿冠处微凹，下缘在齿根处由于齿带发育而明显凸起。由于上缘近齿冠处下凹而下缘平直，使得牙齿的齿冠明显向前上方翘起，齿根直。齿冠和齿根的界线自后上斜向前下方。远中侧棱脊形，近中侧棱不显(NWUV 1486, 图3)。已磨耗的老年标本上，其磨耗面为双侧向内倾斜的长椭圆形，有弱发育的近中侧棱。齿冠前后长33 mm,

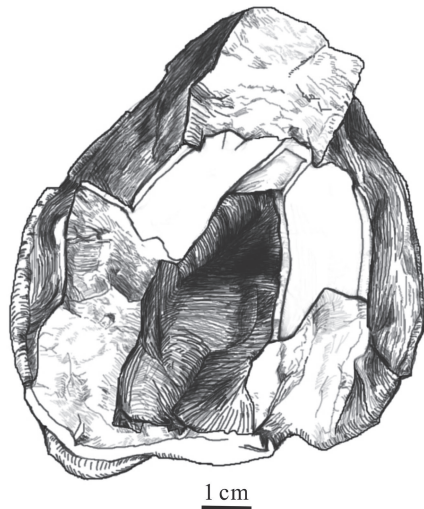


图2 黄河巨犀M3冠面观(NWUV 1482)  
Fig. 2 Line drawing of M3 of *Paraceratherium huangheense* sp. nov. (NWUV 1482)  
in occlusal view

最高处为39 mm, 側向最大宽(厚度)为 25.5 mm (NWUV 1479, 图1D)。

p2 (NWUV 1479, 图1D)个体小, 单根。由于强烈磨蚀, 冠面除前后及唇侧的珐琅质轮廓外, 没有其他齿褶痕迹, 舌侧已磨蚀至齿质。冠面轮廓近于长条形。唇侧齿带发育。

p3 (图1D)轮廓近梯形, 前窄后宽。由于磨耗很深, 冠面只能见到舌侧下跟凹的残余, 下外中谷也只是一个微弱的齿凹。内外齿带发育, 舌侧前半部分齿带已磨蚀掉, 仅有后半部分保留。

p4 (图1D)磨蚀程度深, 只能观察到下三角凹在舌侧的残余, 下跟凹为浅的U字形, 下原脊、下次脊和下后脊很宽, 下内脊向舌侧变得很窄。下外中谷宽缓。内外齿带发育, 唇侧齿带中部低凹, 向后升起。

m1 (图1D)磨蚀很深, 下三角凹在舌侧仅剩一微弱痕迹, 下跟凹为一浅V字形谷, 下外中谷为一宽缓的V形凹坑。下原尖和下后尖膨大, 下前尖最小。下次尖后外侧和下内尖后内侧强烈磨蚀, 分别已经深入齿根和接触到齿根。唇侧齿带在下外中谷处强烈发育。

m2 (图1D)磨耗较轻, 冠面完整。下前尖形成很薄的横脊, 顶端锐, 略向后弯, 向舌侧缓慢下降; 下后脊和下内脊宽度接近, 下三角凹和下跟凹均为U字形, 只是前者宽浅而后者相对窄深。下外中谷为浅V字形。唇侧齿带中前部高而后部低。

m3 (图1D)磨耗最轻, 冠面形态类似于m2。但其下跟凹更宽, 下外中谷更深, 使其横脊比m2稍窄。唇侧齿带仅在前外角处发育, 唇侧后部齿带很弱。牙齿后部即下内脊后壁外侧齿带发育。

NWUV 1480, NWUV 1484与正型(NWUV 1479)的磨蚀程度大致相当, 构造部位可以互补, 推测这三者可能属于同一个体。

**比较与讨论** 自20世纪初以来, 陆续报道了一批在中国各地发现的、保存程度不同的巨犀化石(Teilhard de Chardin, 1926; 杨钟健、周明镇, 1956; 周明镇, 1958; Chow and Xu, 1959; 邱占祥, 1962; 周明镇、邱占祥, 1963, 1964; 邱占祥, 1973; 周明镇等, 1974; 王景文, 1976; 徐余瑄、王景文, 1978; 齐陶、周明镇, 1989; 叶捷等, 2003; 邱占祥等, 2004), 邱占祥、王伴月(2007)对中国已经发现的巨犀化石进行了系统总结。

巨犀亚科包括7个属(邱占祥、王伴月, 2007), 除*Benaratherium*属的情况不明外, 其余主要依吻部构造明显的不同而被分为6个属, 分别为: *Juxia*, 牙式全, 3·1·4·3, i1稍大于其他门齿; *Urtinotherium*, 下齿式全, 3·1·4·3, i1远大于其他门齿; *Paraceratherium*, 仅保留第一对门齿并特别发育, i1向前平伸, 下颌水平支下缘在齿隙下方向上凹入, 下齿式为1·0·3·3; *Dzungariotherium*, 上下颌吻端高度退化, 第一对门齿保留, 但变小, 其他门



图3 黄河巨犀下门齿(NWUV 1486)  
Fig. 3 Photograph of lower incisor of  
*Paraceratherium huangheense* sp. nov.  
(NWUV 1486)

A. mesial view; B. lateral view

犬齿均退失, 水平支下缘自前臼齿下方向前呈弧形上升, 最前端不斜向前下方, 齿式为 $1\cdot0\cdot3\cdot3/1\cdot0\cdot3\cdot3$ ; *Aralotherium*, 吻长, 下门齿及下颌联合部强烈下倾; *Turpanotherium*, 下颌联合部与下门齿i1向前平伸, 左右下门齿间有宽的齿隙(邱占祥、王伴月, 2007)。其中*Paraceratherium*为Forster-Cooper根据发现于巴基斯坦俾路支斯坦德拉布格蒂渐新世沉积中的一件下颌建的一属, 属型种即*P. bugtiense*, 其独特之处是具有互相紧靠而向前方(轻微向下)伸出的加大的第一对下门齿(Forster-Cooper, 1911)。

兰州盆地新发现的巨犀下颌骨(图1, 4A)在形态上与巨犀属*Paraceratherium*最为接近, 特别是其下颌吻部(图4A), 齿缺部分向上弯曲、门齿前伸、水平支下缘平直等特点与建属的模式种*P. bugtiense* (Forster-Cooper, 1911)相当类似(图4B), 而与其他各属明显不同, 因此, 新标本应属于巨犀属。

前人研究认为, 巨犀属包括4个种: 模式种*P. bugtiense*, *P. asiaticum*, *P. grangeri*及*P. lepidum* (图4B-E) (邱占祥、王伴月, 2007)。黄河巨犀和它们都有一定的相似性, 如前伸的门齿, 位于齿列下前方单一的下颏孔, 平直的水平支下缘, 明显的下颌角, 相同的齿式, 较大的尺寸等(表1-3), 但也存在明显的差异(图4; 表4)。

表1 几种巨犀上牙测量比较

Table 1 Measurements and comparison of upper cheek teeth of some paraceratheres (mm)

		<i>P. huangheense</i>	<i>P. asiaticum</i> <sup>1)</sup>	<i>P. grangeri</i> <sup>2)</sup>	<i>P. lepidum</i> <sup>3)</sup>
P2	L	56.1	43.0	45.0	47.8
	W	63.6	51.0	57.8	59.8
P3	L	70.1	55.0	57.8	63.4
	W	87.0	70.0	83.5	87.0
P4	L	79.7	61.0	59.7	69.0
	W	105.5	78.0	93.7	94.8
M2	L	98.2	94.0	95.0	102.3
	W	123.9	93.0	102.8	112.3
M3	L	88.5	96.0	111.0	122.0
	W	113.0	88.0	88.0	107.0
P2-P4	L	176.6	156.0*	179.0	171.0

Based on: 1) Borissiak (1923); 2) Osborn (1923); 3) Qiu and Wang (2007). \* calculated from figure (Borissiak, 1923:l7, fig. 1).

表2 几种巨犀下颌测量比较

Table 2 Measurements and comparison of mandibles of some paraceratheres (mm)

		<i>P. huangheense</i>	<i>P. grangeri</i> <sup>1)</sup>	<i>P. bugtiense</i> <sup>2)</sup>	<i>P. lepidum</i> <sup>3)</sup>
i1-p2 diastema	L	93	127	97	115
Symphysis	L	230	212	152	
Symphysis	min W	81	95	73	
Height at p2		142	131	88	110
Height at m1		139	144	123	130
p2-m3 L		415	400	325	425
p2-p4 L		140	145	122	158
m1-m3 L		268	254	211	265
p2-p4 L/m1-m3 L		0.52	0.57	0.58	0.60

Based on: 1) Granger and Gregory (1936); 2) Forster-Cooper (1911); 3) Qiu and Wang (2007).

表3 几种巨犀下牙齿测量比较

Table 3 Measurements and comparison of lower teeth of some paraceratheres (mm)

	<i>P. huangheense</i>	<i>P. bugtiense</i> <sup>1)</sup>	<i>P. grangeri</i> <sup>2)</sup>	<i>P. lepidum</i> <sup>3)</sup>
i1 crown H×W	39×25.5	57×34	45×39	45×33.5
p2 L	34.52	29	33.5	35.5
W	22.44	18	23.8	22.8
p3 L	48.21	48	51.2	51.6
Anterior W	29.9		37	31.2
Posterior W	39.9	37	41	42.4
p4 L	62.3	57	56.6	65
Anterior W	45.9		42.2	49
Posterior W	55.6	45	42	54.5
m1 L	78.5	58	77	72.7
Anterior W	56.6			56.2
Posterior W	59.8	45	55	
m2 L	95.9	70	92	
Anterior W	66.3			
Posterior W	65.6	45	60	
m3 L	93.0	79	89	
Anterior W	60.6	49	55	
Posterior W	57.3			

Based on: 1) Forster-Cooper (1911); 2) Granger and Gregory (1936); 3) Qiu and Wang (2007). Height on i1: major axis, superolateral-inferomesial in direction.

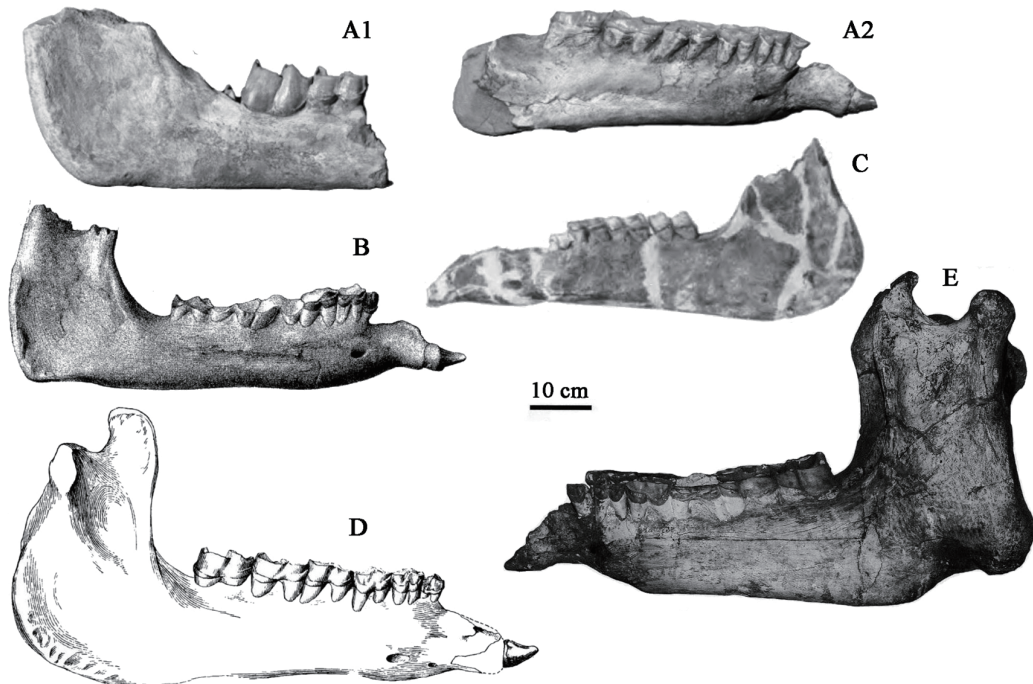


图4 巨犀下颌形态比较

Fig. 4 Morphological comparison of mandible of *Paraceratherium*

A. *P. huangheense*: 1. NWUV 1483, 2. NWUV 1479; B. *P. bugtiense* (Forster-Cooper, 1911); C. *P. asiaticum* (Gromova, 1959); D. *P. grangeri* (Granger and Gregory, 1936); E. *P. lepidum* (邱占祥、王伴月, 2007)

黄河巨犀(图4A1)与布格蒂巨犀*P. bugtiense* (Forster-Cooper, 1911)都缺失P1, P2冠面轮廓也相同, 其下颌(图4B)的吻部形态相当接近, 特别是其p2前的齿缺部分都向上隆起, 向前平伸的两个门齿也略微上翘, 两者下颌角整体形状也接近。两者的主要区别在于: 垂直支后缘斜形态、下颏孔位置以及个体大小的差别(图4A, B; 表4)。

亚洲巨犀*P. asiaticum*的早期材料中未见下颌标本(Borissiak, 1923), 但在Gromova (1959)的研究中有一件*Indricotherium transouralicum*的下颌标本(图4C), 按邱占祥、王伴月(2007)的研究, *I. transouralicum*是*P. asiaticum*的同物异名。新标本与*P. asiaticum*下颌(图4C) (Gromova, 1959)相比, 其主要区别在于后者下颌垂直支后缘的倾斜方向、P2的冠面形态以及下颏孔位置不同(图4A, C; 表4)。

Granger and Gregory (1936)的报道中有较好的葛氏巨犀*Baluchitherium grangeri*的下颌标本(图4D), Gromova (1959)将其归入*I. asiaticum*, 邱占祥、王伴月(2007)研究认为, 它应该独立成种, 并归入巨犀属, 即*P. grangeri*。黄河巨犀与葛氏巨犀相比, 相似之处在于两者大小相近, 都缺失P1, 水平支前端都有一个短粗的下门齿向前伸出。其区别在于下颌角的形态、P2的冠面形态、p2的齿根数目等的差异, 最大的区别在于齿式不同(图4A, D; 表4)。

新疆发现的美丽巨犀*P. lepidum*包含相当完整的下颌骨(图4E), 其吻部也是巨犀属的典型形态(邱占祥、王伴月, 2007)。黄河巨犀与美丽巨犀最大差别在于其缺乏后者下颌下缘在角部之前很深的血管切迹(图4A, E)。

在甘肃皋兰县黄羊头南坡坪动物群的黄砂岩中, 曾发现过巨犀化石(IVPP V 3322, V 3269), 被定为*Paraceratherium* sp. (邱占祥、王伴月, 2007), 推测与本次的化石为同一层位。标本为一件不完整下颌骨, 保留右水平支和左水平支p4前的部分, 联合部前端破碎; m1脱落, 该位置的颌骨部分呈病态收缩。其p2小, 单根, 下颏孔在p3前齿根下方等特征类似于黄河巨犀, 但其m3的下次脊更偏向唇侧。

在兰州盆地还发现有一些零散的巨犀牙齿: V 3317, 属于同一个体的右p3–p4; V 3318, 可能与V 3317为同一个体的左m3; V 3319, 左P4; V 3320, 右m2; V 3321, 左m3。上述化石均产自咸水河中段底部含张家坪动物群的白砂岩层中, 时代为中新世早期(邱占祥等, 1997; Qiu et al., 2001)。p3 (V 3317)近三角形, 前面没有与p2接触的痕迹, 推测齿列没有p2; 下原脊外壁有沟, 舌侧齿带很发育; 下臼齿(V 3320, V 3321)齿冠高, 三角座呈U形, 下前脊长, 与下后脊平行, 三角凹浅而窄, 稍经磨耗即变为一条窄缝, 这些特征和其他各类大巨犀都有明显区别。因此, 上述牙齿被归入秀丽吐鲁番巨犀*Turpanotherium elegans* (邱占祥、王伴月, 2007)。它们在齿式、牙齿形态及地层时代等特征上均与黄河巨犀有较大差别。

下颌标本NWUV 1485与黄河巨犀模式标本和其他巨犀下颌骨均有差异(图1E), 水平支后部下缘有向下斜伸的趋势, m3下跟凹与m2相比明显变窄(图1E1), 而黄河巨犀m3下跟凹则变宽(NWUV 1479, 图1D2), 下颌骨及其牙齿在整体上也显得更为粗壮。目前还难以最终确定这些差别是性别的差异还是种间的变异。因NWUV 1485和其他黄河巨犀材料均采自同一地点和层位, 又有一定的相似性, 如尺寸大小接近, 水平支下缘前部平

直, 下臼齿下外中谷V形, 下跟凹U形等, 暂将其归入黄河巨犀。

黄河巨犀与其他巨犀种的鉴别特征归纳如下(表4):

表4 黄河巨犀与其他巨犀种的主要鉴别特征比较

Table 4 Comparison of *Paraceratherium huangheense* sp. nov. and some *Paraceratherium*

	<i>P. huangheense</i>	<i>P. bugtiense</i> <sup>1)</sup>	<i>P. asiaticum</i> <sup>2)</sup>	<i>P. grangeri</i> <sup>3)</sup>	<i>P. lepidum</i> <sup>4)</sup>
P2 outline	triangular	triangular	trapezoid	trapezoid	triangular
Antecrochet of upper molars	large	clear	weak	very weak	clear
Diastema between i1	present	absent		not close	not close
Root of p2	single	single		double	single
Entolophid of p3-p4	ridgelike	fully formed	entoconid isolated	weakly ridgelike	fully formed
Position of mandibular foramen	below p3	underlies p2	underlies p2		underlies p2
Posterior border of ascending ramus	posteriorly slanted	vertical	anteriorly slanted	anteriorly slanted	vertical
Mandibular angle	angular	angular	rounded	rounded	processlike
Incisura vasorum anterior to the mandibular angle	absent	invisible	invisible	invisible	present
p2-m3 L (mm)	415	325	320	400	425
Dental formula	??33/1033	11(0)43/1033	/1033	1143/1033	1033/1033

Based on: 1) Forster-Cooper (1911) and Gromova (1959); 2) Borissiak (1923) and Gromova (1959); 3) Osborn (1923) and Granger and Gregory (1936); 4) Qiu and Wang (2007).

近年来, 在土耳其其中北部安纳托利亚晚渐新世(Antoine et al., 2008)及土耳其东部渐新世和中新世沉积中(Sen et al., 2011)也发现了一些大巨犀的残破肢骨, 均被记为巨犀未定种*Paraceratherium* sp., 由于没有任何牙齿材料, 难以与黄河巨犀进行比较。

从下颌形态比较可以明显看出, 兰州盆地发现的黄河巨犀与上世纪初发现于巴基斯坦俾路支斯坦中部德拉布格蒂地区的大巨犀模式种*P. bugtiense*最为接近, 因此也显示出两者可能具有比较近的亲缘关系。由于兰州盆地黄河巨犀的地层时代有比较可靠的古地磁数据(岳乐平等, 2000; 张鹏, 2015), 因此可以对亲缘关系较近的、大巨犀模式种产地的地层年代进行合理推测。

长期以来, 俾路支斯坦中部德拉布格蒂产大巨犀化石的地层的时代都被认为是中新世(邱占祥、王伴月, 2007)。由于大量中新世的哺乳动物化石和大巨犀混淆在一起, 对于产大巨犀的层位的年代有人认为早于21~22 Ma, 有人认为是21~18.3 Ma, 有人甚至认为大约在16.5 Ma。法国的古生物学家和巴基斯坦俾路支大学合作, 对该地区进行了相当规模的考察, 在产大巨犀的层位发现了大量的小哺乳动物化石, 如欧洲早渐新世的仓鼠化石*Pseudocricetodon*和*Atavocricetodon*等(Marivaux et al., 1999), 据此推测, 产大巨犀的布格蒂段地层应为下渐新统。本文兰州盆地早渐新世晚期韩家井组底部黄河巨犀的古地磁年代为31.5 Ma, 这为确定巴基斯坦的大巨犀的年代提供了间接的证据, 支持了布格蒂段地层的时代为早渐新世。

兰州盆地的巨犀化石曾经被作为青藏高原在渐新世时尚未隆升到影响大型动物迁徙的有效高度(Deng and Ding, 2015)的主要证据, 本文黄河巨犀的发现可进一步将这一证据的属种明确为巨犀属*Paraceratherium*中的黄河巨犀*P. huangheense*和亲缘关系较近的布格蒂巨犀*P. bugtiense*, 地点明确为高原东北侧的中国兰州盆地和高原西南侧的巴基斯坦德拉布格蒂, 时间限定到渐新世早期大约31.5 Ma左右。

### 3 结论

(1) 兰州盆地韩家井组黄色砂岩近底部发现一巨犀新种：黄河巨犀，其时代为早渐新世晚期，古地磁年代为31.5 Ma。其吻部类似于*P. bugtiense*和*P. lepidum*，但下颌角有变化。巨犀的形态比以前认识的可能更为复杂，存在吻部类似而下颌角差异较大的不同种类。

(2) 兰州盆地发现的黄河巨犀与巴基斯坦的*P. bugtiense*的下颌形态相当类似，两者可能存在较近的亲缘关系。

(3) 黄河巨犀的发现与研究进一步明确了在渐新世早期，青藏高原尚未隆升到可以影响大型哺乳动物自由迁徙的有效高度。

**致谢** 褒心感谢两位审稿人的意见和建议。感谢 Prof. Robert F. Diffendal, Jr. 帮助修改英文提要，张宏发高级工程师参加野外化石发掘，西北大学赵聚发高级技师修复标本，贲杭生参加了野外发掘及室内整理修复，贲桂云女士对化石的发现、发掘及室内整理做了大量工作，对他们的无私帮助和辛勤劳动，特致以衷心感谢。

### References

- Antoine P O, Karadenizli L, Sarac G et al., 2008. A giant rhinocerotoid (Mammalia, Perissodactyla) from the Late Oligocene of north-central Anatolia (Turkey). Zool J Linn Soc Lond, 152(3): 581–592
- Borissiak A A, 1923. Sur un nouveau représentant des rhinocéros gigantesques de l’Oligocène d’Asie. *Indricotherium asiaticum*, n.g. n.sp. Mém Soc Géol Fr, 59: 1–16
- Chiu C S, 1962. Giant rhinoceros from Loping, Yunnan, and discussion on the taxonomic characters of *Indricotherium grangeri*. Vert PalAsiat, 6(1): 57–71
- Chiu C S, 1973. A new genus of giant rhinoceros from Oligocene of Dzungaria, Sinkiang. Vert PalAsiat, 11(2): 182–191
- Chow M C, 1958. Some Oligocene mammals from Lunan, Yunan. Vert PalAsiat, 2(4): 263–267
- Chow M C, Chiu C S, 1963. New genus of giant rhinoceros from Oligocene of Inner Mongolia. Vert PalAsiat, 7(3): 230–239
- Chow M C, Chiu C S, 1964. An Eocene giant rhinoceros. Vert PalAsiat, 8(3): 264–268
- Chow M C, Xu Y X, 1959. *Indricotherium* from Hami Basin, Sinkiang. Vert PalAsiat, 3(2): 93–98
- Chow M C, Chang Y P, Ting S Y, 1974. Some Early Tertiary Perrisodactyla from Linan Basin, E. Yunnan. Vert PalAsiat, 12(4): 262–278
- Deng T, Ding L, 2015. Paleoaltimetry reconstructions of the Tibetan Plateau: progress and contradictions. Natl Sci Rev, 2: 417–437
- Forster-Cooper C, 1911. *Paraceratherium bugtiense*, a new genus of Rhinocerotidae from the Bugti Hills of Baluchistan: preliminary notice. Ann Mag Nat Hist, 8: 711–716
- Granger W, Gregory W K, 1936. Further notes on the gigantic extinct rhinoceros *Baluchitherium*, from the Oligocene of Mongolia. Bull Am Nat Hist, 72(1): 1–73
- Gromova V, 1959. Giant rhinoceroses. Tr Paleont Inst, 71: 1–164

- Li Z C, Li Y X, Zhang Y X et al., 2016. Nanpoping fauna of the Lanzhou Basin and its environmental significance. *Sci China Earth Sci*, 59: 1258–1266
- Lucas S G, Sobus J, 1989. The systematics of indricotheres. In: Prothero D R, Schoch R M eds. *The Evolution of Perissodactyls*. New York: Oxford University Press. 358–378
- Marivaux L, Vianey-Liaud M, Welcomme J L, 1999. Première découverte de Cricetidae (Rodentia, Mammalia) oligocènes dans le synclinal sud de Gandoï (Bugti Hills, Balouchistan, Pakistan). *C R Acad Sci Paris*, 329: 839–844
- Osborn H F, 1923. *Baluchitherium grangeri*, a giant hornless rhinoceros from Mongolia. *Am Mus Novit*, 78: 1–15
- Qi T, Zhou M Z, 1989. A new species of *Juxia* (Perissodactyla), Nei Mongol. *Vert PalAsiat*, 27(3): 205–208
- Qiu Z X, Wang B Y, 2007. Paraceratheres fossils of China. *Palaeont Sin, New Ser C*, 29: 1–396
- Qiu Z X, Wang B Y, Qiu Z D et al., 1997. Recent advances in study of the Xianshuihe Formation in Lanzhou Basin. In: Tong Y S, Zhang Y Y, Wu W Y et al. eds. *Evidence for Evolution: Essays in Honor of Prof. Chungchien Young on the Hundredth Anniversary of His Birth*. Beijing: China Ocean Press. 177–192
- Qiu Z X, Wang B Y, Qiu Z D et al., 2001. Land mammal geochronology and magnetostratigraphy of mid-Tertiary deposits in the Lanzhou Basin, Gansu Province, China. *Eclogae Geol Helv*, 94: 373–385
- Qiu Z X, Wang B Y, Deng T, 2004. Indricotheres (Perissodactyla, Mammalia) from Oligocene in Linxia Basin, Gansu, China. *Vert PalAsiat*, 42(3): 177–192
- Sen S, Antoine P O, Varol B et al., 2011. Giant rhinoceros *Paraceratherium* and other vertebrates from Oligocene and Middle Miocene deposits of the Kagizman-Tuzluca Basin, Eastern Turkey. *Naturwissenschaften*, 98(5): 407–423
- Teilhard de Chardin P, 1926. Description de mammifères Tertiaires de Chine et de Mongolie. *Ann Paléont*, 15: 1–52
- Wang J W, 1976. A new genus of Forstercooperinae from the Late Eocene of Tongbo, Henan. *Vert PalAsiat*, 14(2): 104–111
- Xie G P, 2004. The Tertiary and local mammalian faunas in Lanzhou Basin, Gansu. *J Stratigr*, 28: 67–80
- Xu Y X, Wang J W, 1978. New materials of giant rhinoceros. *Mem Inst Vert Paleont Paleoanthrop*, 13: 132–140
- Ye J, Meng J, Wu W Y, 2003. Discovery of *Paraceratherium* in the northern Junggar Basin of Xinjiang. *Vert PalAsiat*, 41(3): 220–229
- Young C C, Bien M N, 1937. Cenozoic geology of the Kaolan-Yungteng area of central Kansu. *Bull Geol Soc China*, 16: 221–260
- Young C C, Chow M C, 1956. Some Oligocene mammals from Lingwu, N. Kansu. *Acta Palaeontol Sin*, 4(4): 447–459
- Yue L P, Heller F, Qiu Z X et al., 2001. Magnetostratigraphy and palaeoenvironmental record of Tertiary deposits of Lanzhou Basin. *Chin Sci Bull*, 46: 770–773
- Zhang P, 2015. Magnetostratigraphy and paleoenvironmental evolution of the Middle Eocene-Early Miocene deposits in the Lanzhou Basin, northwest China. Ph. D thesis. Xi'an: Institute of Earth Environment. 1–117